Edge Truncation Effects in a Wide-Scan Phased Array of Connected Bowtie Antenna Elements

Citation for the original published paper (version of record):

Khanal, P., Yang, J., Ivashina, M. et al (2020). Edge Truncation Effects in a Wide-Scan Phased Array of Connected Bowtie Antenna Elements. 14th European Conference on Antennas and Propagation, EuCAP 2020: 1-5. http://dx.doi.org/10.23919/EuCAP48036.2020.9135245

Edge Truncation Effects in a Wide-Scan Phased Array of Connected Bowtie Antenna Elements

Prabhat Khanal[1], Jian Yang[1], Marianna Ivashina[1], Anders Höök[2] and Ruoshan Luo[2]

[1] Department of Electrical Engineering, Chalmers University of Technology, Gothenburg, Sweden
prabhat@chalmers.se, jian.yang@chalmers.se, marianna.ivashina@chalmers.se
[2] SAAB AB, Gothenburg, Sweden
anders.hook@saabgroup.com, ruoshan.luo@saabgroup.com

***Abstract*—Edge truncation effects are critical when designing a phased array, as these can lead to the variation of the active antenna impedance and radiation pattern between individual array elements. This paper investigates edge truncation effects in an array of connected Bowtie antenna elements that has been initially designed through an infinite array approach. This design represents a novel implementation of the connected-array concept that offers a wide-scan performance with up to $\pm$ 80° scan range in the E-plane (in the infinite array). The goal of this study is to estimate the minimum size of a realistic finite array of such connected Bowtie antennas.**

***Index Terms*—phased array, connected antenna array, Bowtie antenna array, edge truncation effects, finite array, semi-infinite array.**

I. Introduction

Phased-array antennas with a high gain, wide bandwidth, and wide-scan capabilities are in demand for many applications, such as radars and wireless communication. A common approach of designing such arrays is to first optimize the antenna element for an infinite array scenario using the Floquet's theorem [1], and then fine-tune its geometry by using a more accurate (though more computationally expensive) modeling technique. The infinite array approach implies that the impact of the edge truncation effects (ETEs) on the array performance is negligible. This approach is usually a reasonable assumption for phased arrays which exhibit relatively weak antenna mutual coupling effects and are designed to operate within a limited scan-angle range [2].

However, for wide-scan applications, the edge truncation effects can significantly modify the antenna characteristics (e.g., active reflection coefficient and embedded element patterns) compared to the predictions for the infinite array [3]. There are mainly three factors causing these differences: (i) the excitation of the array antenna is spatially truncated, as compared with the Floquet-mode excitation; (ii) the geometrical features of the array near the edges, such as the ground plane, radome, and antenna element shape, play a dominant role in the performance of the edge elements; and (iii) the standing wave pattern over the aperture, resulting from the multiple reflections of the attenuated guided waves from the edges [4]. All these factors are specific to the array antenna element type and the array dimensions and typically exacerbate at large scan angles from broadside [5]. In practice, an accurate electromagnetic analysis is required to capture these effects.

To some extent, the impact of the ETEs on the antenna active impedance can be minimized by applying the antenna element excitation distribution that is tapered towards the array edge [6]. However, this approach is not suitable for the applications where the power amplifiers (PAs) or low noise amplifiers (LNAs) connected to the antenna elements are required to operate at equal power levels, to achieve maximum power efficiency or minimum noise temperature, while minimizing the non-linear distortion effects between PAs and noise coupling effects between LNAs that can occur in connected arrays [7].

In this work, we investigate the ETEs in terms of the standing wave pattern over the array aperture, defined by the magnitude of the active reflection coefficients of the array antenna elements which are located in the scan plane. We study this problem numerically by using a full-wave electromagnetic simulator CST Studio Suite [8] and compare the performance of the antenna elements in the middle of the array (that are expected to behave as in the infinite array) to the elements near the edge. In this study, the scale of the array is varied from a few to 50 elements in the scan plane.

II. Antenna design

Fig. 1 shows the array antenna under study, which has been proposed in [9] and designed through the infinite array approach in CST Studio Suite. It is a horizontally polarized S-band (3 GHz) array consisting of 20×200 (vertical$\times$ horizontal) Bowtie antenna elements. The infinite array simulations predict the required scan performance which is satisfied within up to $\pm 80°$ off the broadside in the E-plane, where the active reflection coefficient (Γ_{act}) is better than -10 dB and -5 dB over the bandwidth of 10% and 25%, respectively (see Fig. 2).

In comparison with the original element design in [9], we have introduced the shoulders at the edges of the Bowtie arms to further increase the desired scan performance ($|\Gamma_{act}|$ <-10

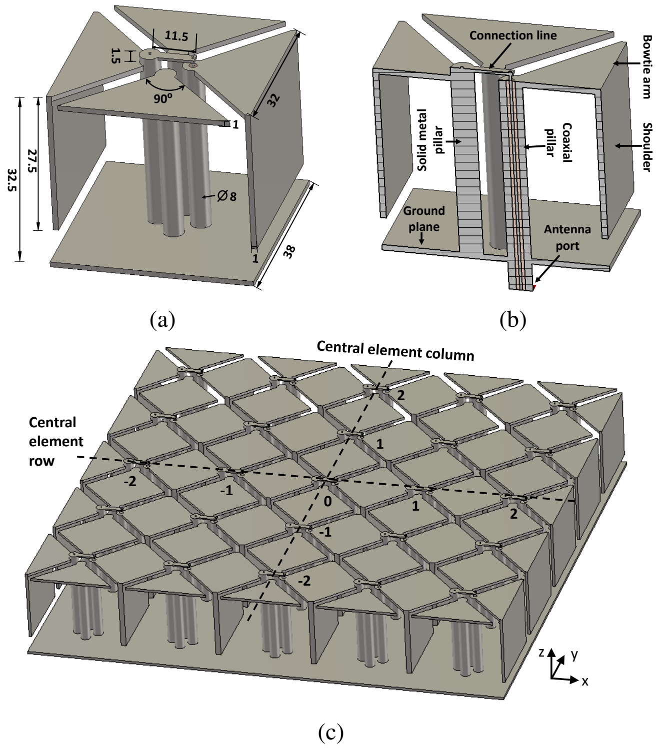

Fig. 1: (a)-(b) The geometry of the cross Bowtie antenna element in different views, and (c) a 5×5 array antenna model. The standard IEEE polarization definition (Ludwig 3) is used.

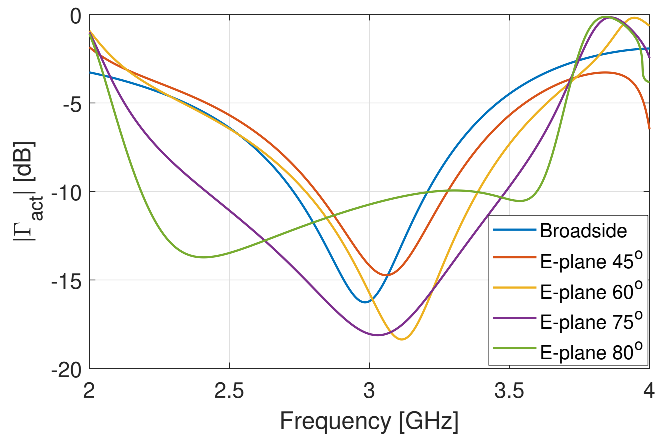

Fig. 2: The active reflection coefficients of the uniformly excited infinite phased array at various scan angles.

dB) in the E-plane from $\pm 75°$ to $\pm 80°$ for the infinitely large array. Furthermore, the element spacing for the present design in both the E- and H-planes is 38 mm (i.e. 0.43 λ_{max}, where λ_{max} =3.375 GHz).

The details of the element design are the following:

- The array element is composed of two orthogonal Bowtie elements which are placed above the ground plane and supported by three solid pillars and one coaxial pillar. The coaxial pillar has the function of the coaxial feed line of 50 Ω impedance, where the outer conductor is connected to the ground plane at one end and to one arm of a bowtie at the other end, while its inner connector is connected to the other arm of the same Bowtie via a metal line (referred to as the connection line in Fig. 1b). The Bowtie arm connected with the inner conductor is also connected to the ground via the solid pillar. These coaxial-solid pillar pair thus represent a balun structure which transforms the single-ended antenna ports to the differential ports of the Bowtie antenna.
- The arms of the second Bowtie are connected with a pair of solid pillars to the ground. If the dual-polarization is desired, one can configure the second Bowtie with a pair of the coaxial-solid pillar, similarly to the first Bowtie. It is worth mentioning that removing the second Bowtie reduces the bandwidth of the antenna element in the infinitely large array. Therefore, even though only the horizontal polarization is required for the considered application, the second Bowtie is still present in the element in this work.

III. Semi-infinite array analysis to study ETEs

To study the edge truncation effects in large-scale arrays, we have applied a semi-infinite array approach where the array is periodic in one direction and finite in the orthogonal one. This significantly relaxes the computational time while keeping the analysis rather simple. In this approach, it is expected that the elements in the middle of the semi-infinite array have similar active impedance performance to that of the elements in the infinite array case. Furthermore, we follow the hypnotizes that if the elements in the middle of the semi-infinite array of size $\infty \times y$ and the elements of the semi-infinite array of size $x \times \infty$ behave similarly to that of the elements in infinite array of size $\infty \times \infty$, there is a reasonable chance that the elements of a large scale finite array of size $x \times y$ would also behave similar to the elements in the infinite array.

A. Infinite in the E-plane and Finite in the H-plane

In this sub-section, the semi-infinite arrays of $\infty \times 3$, $\infty \times 7$, $\infty \times 11$, $\infty \times 15$ and $\infty \times 21$ antenna elements are studied, where the '∞' symbol is referred to the E-plane, which is realized by using a unit cell in the x-direction with periodic boundary. Fig. 3 shows the active reflection coefficients at 3 GHz across the y-direction elements of the respective arrays and compares them with that of the infinite array case for the broadside beam. The element numbering shows the position of the elements in the array as indicated in Fig. 1c. Similarly, Figs. 4, 5 and 9 present the same configurations for the beam 45°, 60° and 80° off the broadside, respectively.

Figures 3, 4, 5 and 9 show that due to the edge truncation effects, there are varying magnitude values of the active reflection coefficients across the array in the y-direction, even when the beam scanning is realized along the x-axis. These variations are symmetric around its central elements because

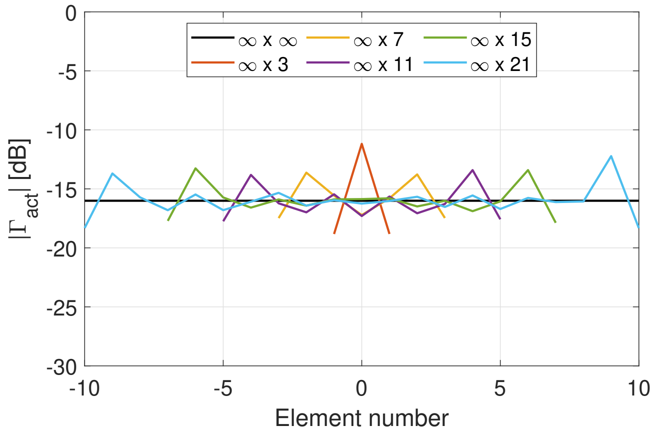

Fig. 3: Active reflection coefficients at 3 GHz at broadside. The array is infinite in E-plane and finite in H-plane. The element numbering is as in Fig. 1.

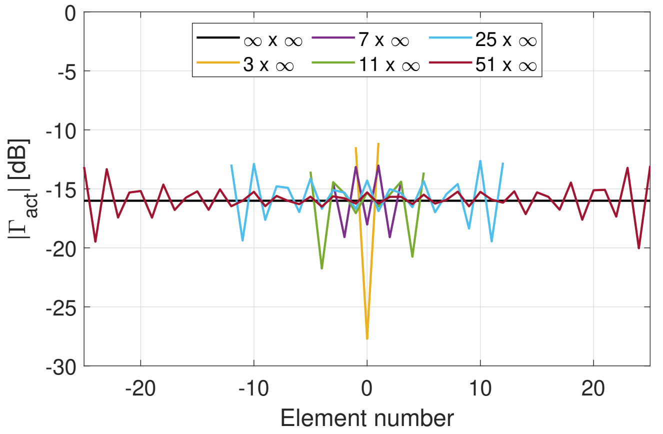

Fig. 6: Active reflection coefficient at 3 GHz at broadside. The array is finite in E-plane and infinite in H-plane. The element numbering is as in Fig. 1.

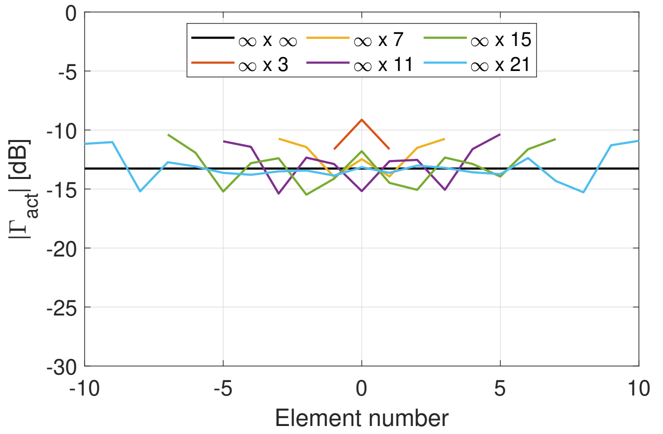

Fig. 4: Active reflection coefficient at 3 GHz at 45° off the broadside. The array is infinite in E-plane and finite in H-plane. The element numbering is as in Fig. 1.

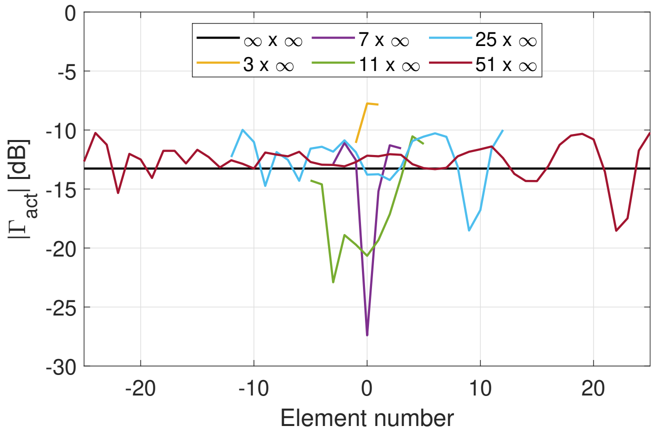

Fig. 7: Active reflection coefficient at 3 GHz at 45° off the broadside. The array is finite in E-plane and infinite in H-plane. The element numbering is as in Fig. 1.

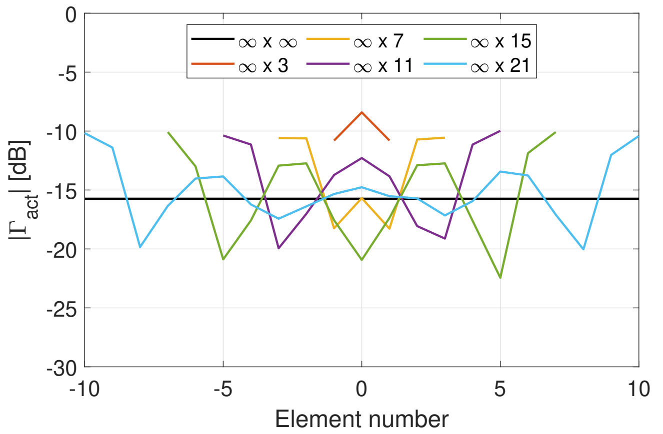

Fig. 5: Active reflection coefficient at 3 GHz at 60° off the broadside. The array is infinite in E-plane and finite in H-plane. The element numbering is as in Fig. 1.

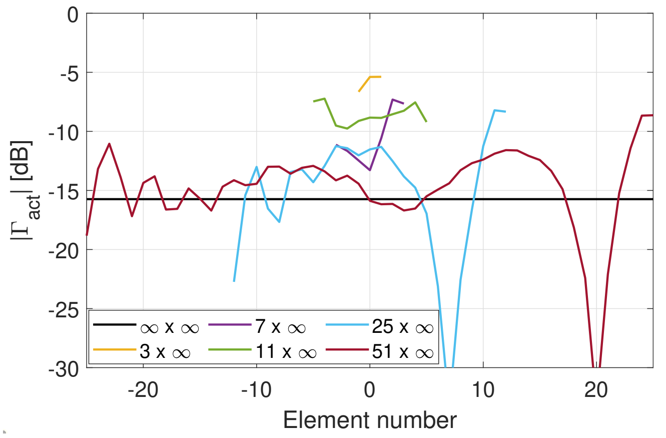

Fig. 8: Active reflection coefficient at 3 GHz at 60° off the broadside. The array is finite in E-plane and infinite in H-plane. The element numbering is as in Fig. 1.

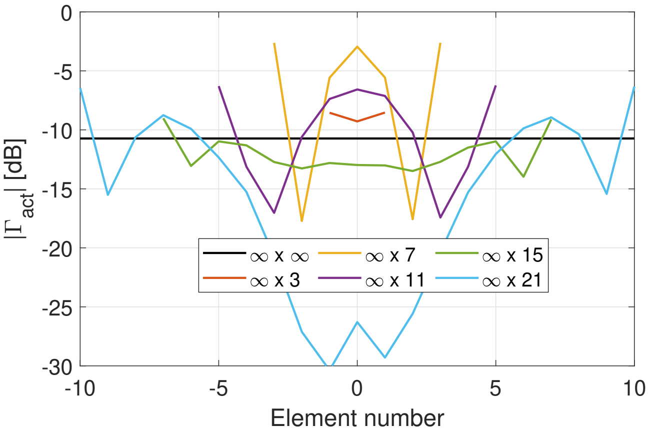

Fig. 9: Active reflection coefficient at 3 GHz at 80° off the broadside. The array is infinite in E-plane and finite in H-plane. The element numbering is as in Fig. 1.

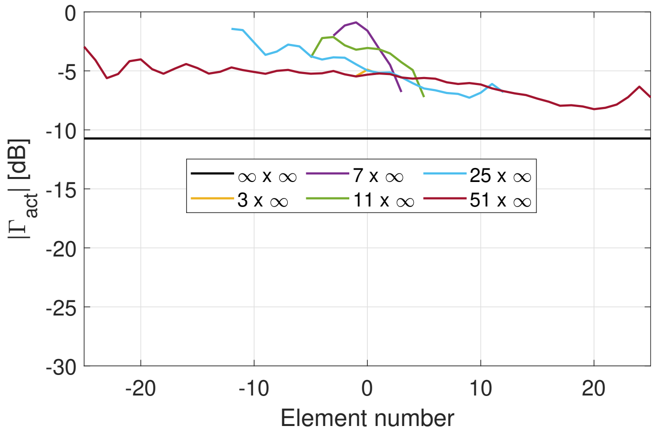

Fig. 10: Active reflection coefficient at 3 GHz at 80° off the broadside. The array is finite in E-plane and infinite in H-plane. The element numbering is as in Fig. 1.

these elements are in the non-scanning direction, and the corresponding symmetrically located elements (symmetric about its central element) have the same mutual coupling environment. It is worth noting that, the impact of the edge truncation effects on the active reflection coefficients are strongly dependent on the scan angle. It is evident that the performance degradation is stronger for the edge elements and reduces towards the middle of the array, while slowly converging to the infinite array case for large-scale arrays. Furthermore, it is seen that the infinite array solution approximates reasonably well the performance of the $\infty \times 11$ element array, both at the broadside and 45° scan angle. For a 60° scan angle, we observe a similar degree of agreement for the $\infty \times 21$ element array. For 80° scan angle, the active reflection coefficients in the middle of the $\infty \times 21$ element array is better than that of an infinite array. The targeted antenna array will have the number of elements in the order of 20 in this direction; hence, larger-scale arrays have not been considered.

B. Finite in E-plane and infinite in H-plane

In this sub-section, the semi-infinite arrays of $3\times\infty$; $7\times\infty$; $11\times\infty$; $25\times\infty$ and $51\times\infty$ antenna elements are studied, where '∞' is defined in the H-plane. Figures 6, 7, 8 and 10 present the simulation results for the same configuration as for the E-plane of sub-section III-A.

The variations of the active reflection coefficient magnitude across the array in x-directions are symmetric about its central element for the broadside, and asymmetric when scanning at 45°, 60° and 80°. It is because these elements are in the scanning direction, and the excitations of the elements have different phases when scanning. Similar to observations of sub-section III-A, the impact of the edge truncation effects depends on the scan angle. The active reflection coefficients of the central elements of $11\times\infty$ elements array have converged well to that of the infinite array at the broadside, and it is better than that of the infinite array at the scan angle 45°. However, at 60° the solutions of the semi-infinite and infinite arrays only partially agree, and become very different for the 80° case.

This outcome of our study points in the direction of the critical factors contributing to the edge truncation phenomena in connected arrays, (as mentioned in section I), and their combined effect:

- the stronger spatial truncation of the array element excitation at larger scan angles in the E-plane, as compared with the Floquet-mode excitation; and
- the proposed antenna element type, which possibility suffers from stronger reflections from its edges for the horizontal polarization when scanning in the E-plane, causing a more pronounced standing wave pattern over the array aperture.

As a consequence, even the $51\times\infty$ element array model is not large enough to approximate the performance of the infinite array. Due to the lack of computational resources, arrays bigger than $51\times\infty$ are not studied in this paper.

IV. Conclusion

The study of the edge truncation effects in the arrays of connected cross Bowtie antenna element has shown that for the broadside beam direction, the one would need an 11×11 element array to reasonably accurately represent the behavior of the antenna active impedance in the infinite array. This observation is consistent with a common engineering rule of thumb of $5\lambda\times5\lambda$ (i.e. 10×10 antenna elements for 3 GHz) [10]. However, the same observation is not valid for wide-angle scanning scenarios. In particular, much larger scale arrays would be required, i.e., 51×21 element array and larger than that, for the 60° and 80° scan directions, respectively.

The next phase of this work could be to study the ways of reducing the edge truncation effects in the finite array for the wide scan angles off the broadside direction.

REFERENCES

[1] G. Floquet, "On the linear differential equations with periodic coefficients," *Scientific journals of the Ecole Normale Supérieurier*, vol. 2nd s, 12, pp. 47–88, 1883.

[2] J. M. Usoff and B. A. Munk, "Edge effects of truncated periodic surfaces of thin wire elements," *IEEE Transactions on Antennas and Propagation*, vol. 42, pp. 946–953, July 1994.

[3] B. A. Munk, *Finite Antenna Arrays and FSS*. A John Wiley & Sons, Inc Publication, 2005.

[4] D. S. Janning and B. A. Munk, "Effects of surface waves on the currents of truncated periodic arrays," *IEEE Transactions on Antennas and Propagation*, vol. 50, pp. 1254–1265, Sep. 2002.

[5] R. C. Hansen and D. Gammon, "Standing waves in scan impedance of finite scanned arrays," *Microwave and Optical Technology Letters*, vol. 8, no. 4, pp. 175–179, 1995.

[6] M. Arts, M. Ivashina, O. Iupikov, L. Bakker, and R. van den Brink, "Design of a low-loss low-noise tapered slot phased array feed for reflector antennas," in *Proceedings of the Fourth European Conference on Antennas and Propagation*, pp. 1–5, April 2010.

[7] M. V. Ivashina, "Joint design and co-integration of antenna-ic systems," in *2019 13th European Conference on Antennas and Propagation (EuCAP)*, pp. 1–7, March 2019.

[8] Dassault Systems, "CST Studio Suite 2019."

[9] P. Khanal, J. Yang, M. Ivashina, A. Hook, and R. Luo, "A wide coverage s-band array with dual polarized connected bowtie antenna elements," in *2019 IEEE International Symposium on Antennas and Propagation USNC/URSI National Radio Science Meeting*, July 2019.

[10] H. Holter and H. Steyskal, "On the size requirement for finite phased-array models," *IEEE Transactions on Antennas and Propagation*, vol. 50, pp. 836–840, June 2002.